

ENHANCEMENT OF SEAT PERFORMANCE IN LOW-SPEED REAR IMPACT

Harald Zellmer
Michael Stamm
Alexander Seidenschwang
Autoliv GmbH, Elmshorn,
Germany
Anton Brunner
Winterthur Insurance Corp., Dep. of Accident Research, Winterthur,
Switzerland
Document No. 231

ABSTRACT

Benchmark testing of existing seat designs reveals poor performance in low-speed rear impacts. In tests according to the test procedure proposed by GdV, ETH and Autoliv, the neck injury criterion NIC exceeds the limiting value of 15 for almost all seats without a CSD protection system. As only few new car models offer this, a system was developed and tested for aftermarket fitting. The Aftermarket Anti Whiplash System, AWS, consists of a yielding device which is fitted to the seat rails and allows the whole seat to rotate and move backwards. This reduces thorax acceleration and thus the NIC value. As the force required to actuate the device depends on the position of the seat, the system offers optimum protection for large and small occupants.

Tests with rear impact dummies (BioRID and HIII(TRID)) show a noticeable reduction in NIC and head rebound speed compared to the standard seat. Loadings to the neck at Δv 15 km/h with AWS are in the same magnitude as at 9 km/h without AWS. MADYMO simulations with real crash pulses have been performed, and the potential benefit of AWS is estimated on the basis of those results.

1. INTRODUCTION

Cervical spine distortion injuries (CSD) in passenger car rear impact accidents, in particular at low speeds with a Δv of 15 km/h or less, are becoming increasingly problematic. To quantify the influence of the car seats on the probability of injury, a testing method for low speed rear impact was developed in a co-operative effort by the GdV Institute for Vehicle Safety, Working Group on Accident Mechanics at University / ETH Zurich and Autoliv Germany /1/. A rear impact with a Δv of 15 km/h and a vehicle deceleration of 6 g is simulated. The dummy used is a Hybrid III 50th Percentile with a TRID neck [HIII(TRID)]. The main evaluation criteria are Neck Injury Criterion NIC, neck moments, and rebound velocity of the head. Over 30

different seat types have now been tested in comparative tests /1/. It was seen that seats with CSD protection systems show much better dummy readings than seats without such systems.

Since only few vehicle models are equipped with a CSD protection system to date, the aim of Autoliv and Winterthur Insurance Corp. was to develop a system for aftermarket vehicle installation, especially because the vehicles being sold today or being only few years old will be on the roads for many more years.

Basically, there are by now two different systems for reduction of CSD injuries on the market: active headrest and yielding backrest. Both of these systems reduce relative movement between the head and thorax in the event of rear impact, see Fig.1. The system with the yielding back rest turns out to be better suited to aftermarket installation. The deformation element that provides controlled energy absorption in the seat back during a rear impact can be integrated in the seat underframe. It is therefore not necessary to dismantle the seat back. An additional advantage of this protection system is the clear reduction of head rebound speed, and it also provides a degree of protection if the head rest is positioned incorrectly or the occupant is not in standard seating position.

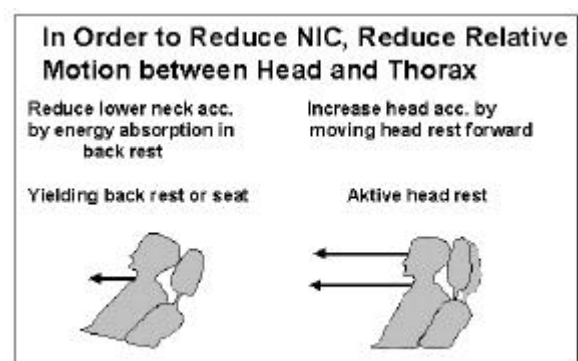


Fig. 1: Function of common CSD protection systems

In the following the function of the system is described, followed by an investigation of which dummy is most suitable for use in optimising the system. The results of sled tests with and without AWS are discussed and the benefit of AWS is investigated by means of MADYMO simulation with real crash pulses.

2. THE CSD PROTECTION SYSTEM AWS

The functional principle of our CSD protection system is based on a defined energy absorption in the back rest. This principle has been employed successfully for a number of years (Fig. 2). In standard series seats, the deformation element is located in the recliner. During rear impact, a parallel backwards movement of the seat back begins at a point of critical load, which motion is then transformed into rotation $/2/$. The backwards movement is limited so that the seat back will offer sufficient protection in a high-speed impact.

Aftermarket installation of an energy-absorbing recliner in an existing seat type appeared unsuitable to us for the following reasons:

- A change in this area might widen the seat and hinder its adjustability,
- The design is limited to a specific seat type,
- The seat cover may have to be cut and covered,
- Installation in a workshop would take too long.

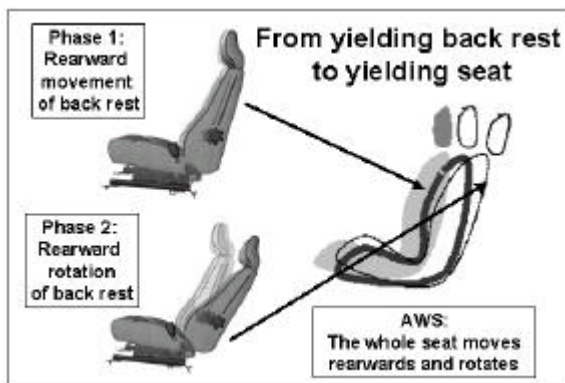


Fig. 2: Seat kinematic during rear impact

Thus, we decided to integrate the deformation element in the seat rail. In this solution, the entire seat moves backwards with the desired motion (see Fig. 2). The deformation element is in the form of a tear-open plate installed in the area of the connection between the vehicle floor and the longitudinal seat adjustment element (see Fig. 3). This connection part is solidly anchored in the floor of the vehicle with the hole frame for the longitudinal seat adjustment in its upper part. In a rear impact, the deformation element

is pulled upwards so that the seat back tips backwards. This particular installation site is also special for another reason: Different levering ratios result from the position of the seat in the longitudinal direction. The CSD protection system is more readily released when the seat is positioned at the front than at the back - a simple mechanical adaptation of the release threshold to the size of the passenger. This means optimum protection for small, lightweight persons as well as large, heavy persons.

The requirement to our system is to release at a defined velocity change of the impacted vehicle and thus reduce neck loadings. On the other hand, the system must not be damaged or caused to release by normal or even extreme everyday loads, e.g. when the rear-seat passenger gets in and out and holds the seat back of the front seat. This stipulation results in a conflict of goals. It was solved by adding a trigger rivet to the deformation element that will withstand a defined stress load. The rivet does not release the mechanism until this stress load point is exceeded.

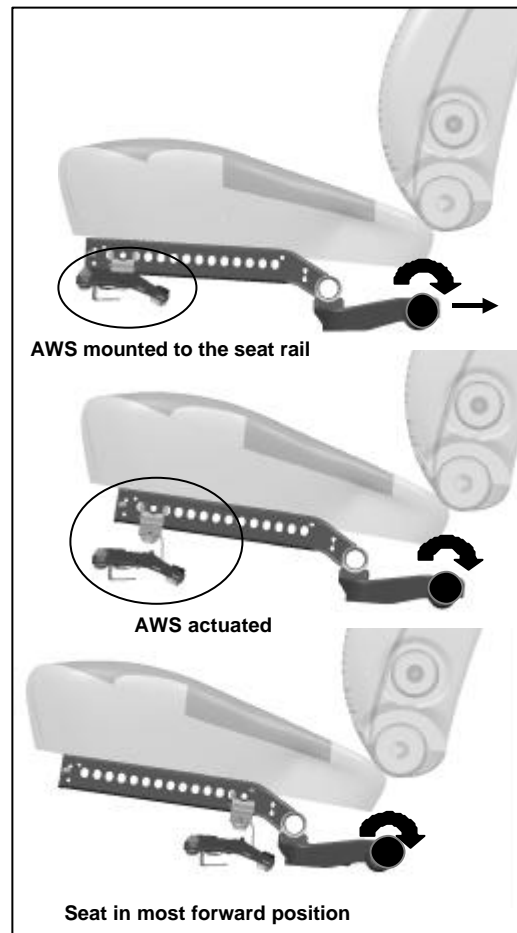


Fig. 3: Sketch showing design principle of AWS

3. DUMMY COMPARISON BioRID /HIII(TRID)

Initial tests with AWS according to the GdV/ETH/Autoliv test method revealed a clear reduction of neck loadings. The relevant parameters NIC, neck moments and head rebound speed were reduced by half. It has to be pointed out that the NIC declined from above 15 to well below 10. According to the test specification, a 50th Percentile Hybrid III Dummy with TRID neck was used in these tests. In optimising the AWS, this dummy appeared unsuitable to us because it reacts with little sensitivity to changes in the properties of the deformation element.

The BioRID has been available for some time as an alternative to the HIII(TRID) /3/. This dummy was specially designed for low-speed rear impact tests. Since it is known that the dummies supply different results /4/, we began by comparing the two dummy types.

The two seat types selected were those that had performed particularly well or poorly in previous tests /1/. The tests were run at 15 km/h and a 6 g rectangular pulse in accordance with the proposed test procedure. Figs. 4 and 5 compare the time histories for the good and bad seat with BioRID and HIII(TRID). With the bad seat, the two dummies showed wide variances, with the maximum NIC values at 26.0 for the BioRID and 18.4 for the HIII(TRID). With the BioRID, the NIC remains near zero for the first 45 ms, then climbs to above 20 in 20 ms. The time history shows pronounced maxima, with the highest in the third and last position. It should be mentioned here that the filtering of the head and of the thorax accelerometer was done at CFC 180, which also applies to the other tests described in this paper with the BioRID. The upward curve with the HIII(TRID) begins at 25 ms, with the NIC climbing almost continuously up to the maximum value, which is reached at 102 ms, 6 ms later than with the BioRID. With the good seat, the curves for both dummies are highly similar, with the corresponding NIC values very close together at 9.0 and 8.5.

Since the NIC is composed of one acceleration and one speed component as:

$$NIC(t) = a_{rel}(t) \cdot 0.2 + (v_{rel}(t))^2,$$

with a_{rel} and v_{rel} being the relative acceleration and speed between head and thorax, it is interesting to investigate how these components turn out with the different dummies. This is shown in figures 6 and 7 for the bad seat. For both dummies, the NIC value is determined by the acceleration component alone up to about 70 ms. The speed component increases with both dummies beginning at 70 ms continuously and

reaches its maximum when the acceleration component reaches a nearly constant level due to head / headrest contact. Whereas the acceleration component with the HIII(TRID) is nearly constant beginning at 80 ms, it drops for the BioRID beginning at 75 ms. For both dummies the acceleration component comprises about 30% of the maximum value. With the good seat, on the other hand, the acceleration component is negligible at the NIC for both dummies.

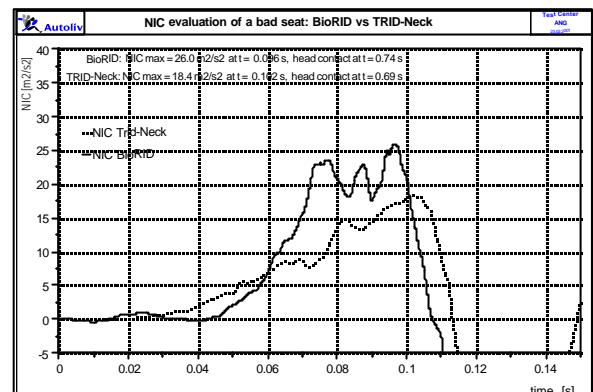


Fig. 4: Time history of NIC, bad seat

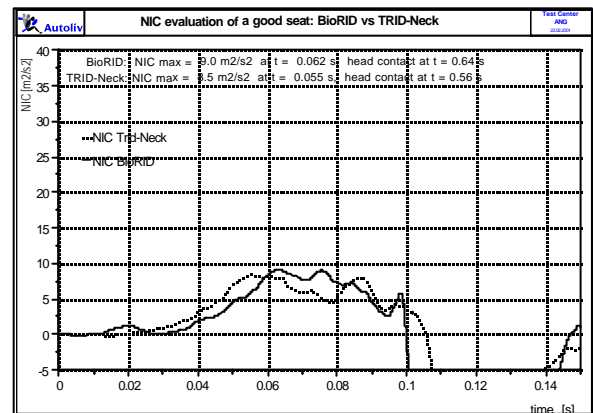


Fig. 5: Time history of NIC, good seat

An interesting picture results from observation of the neck moments. An example of this is seen in Fig. 8: the time history for the bad seat. In general, these figures are much lower with the BioRID. The HIII(TRID) shows a slight flexion prior to head contact with the headrest, which then shows a transition to a pronounced extension following the contact at approx. the greatest backwards point of the head. During rebound, flexion occurs once again. The BioRID shows flexion during the head / headrest contact and during rebound extension. All the values are only a fraction of those for the HIII(TRID). With the good seat, the neck moments measured with the

BioRID are below 2 Nm, both in extension and flexion, for the HIII(TRID) 12.8 Nm and 5.4 Nm. This behaviour can be explained by the much more flexible cervical spine of the BioRID. This results in lower moment at the neck/head transition.

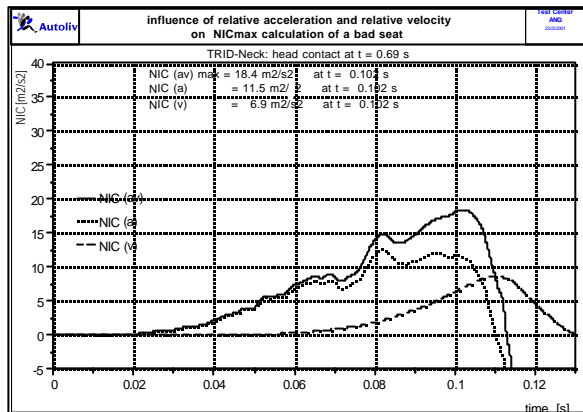


Fig. 6: Speed and acceleration as contributing factors to NIC, bad seat, HIII(TRID)

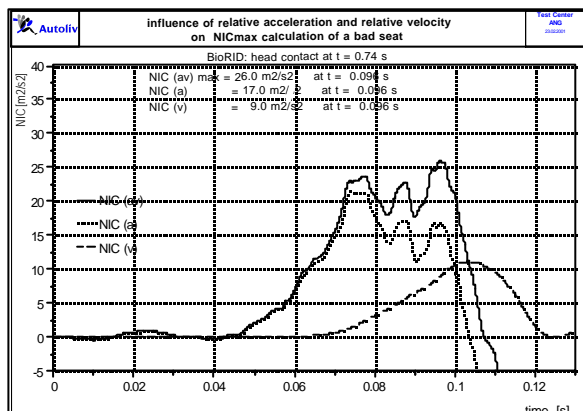


Fig. 7: Speed and acceleration as contributing factors to NIC, bad seat, BioRID

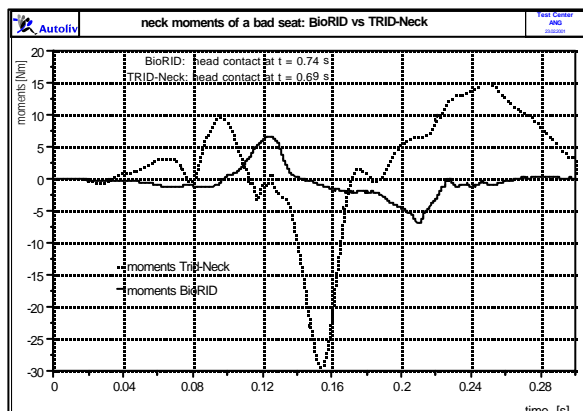


Fig. 8: Neck moments, bad seat

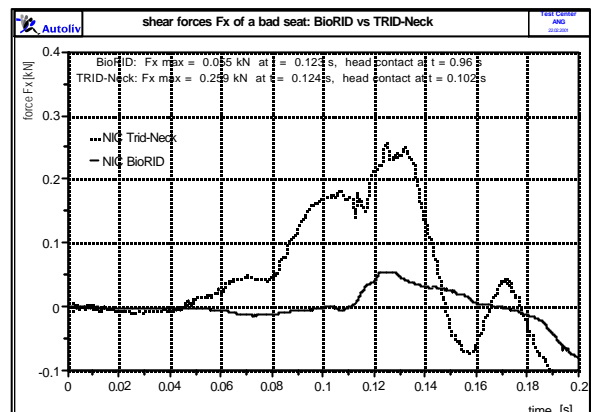


Fig. 9: Shearing forces, bad seat

The shearing forces also show a deviant behaviour pattern. Fig. 9 shows their time history.

Another evaluation criterion in the test method for low-speed rear impact is head rebound speed. This factor is for the BioRID about 30% greater for the two seats tested than for the HIII(TRID). It must be mentioned here that the head rebound speed has been criticized /5/. It has been proposed that the speed of the T1 vertebra be used as the measure for rebound. We will therefore not undertake a further evaluation of the rebound speed at this point.

Which dummy is most suitable for use in optimising the AWS and which criterion should be taken as a basis for optimisation? The neck moments or shearing forces cannot be used for the above reasons. The rebound speed is not a criterion for evaluation of the important first phase prior to headrest contact, so that it makes no sense to optimise in terms of this parameter. The time history of the NIC is similar for both of the dummy types tested, so that this parameter should be used to optimise the system. The BioRID has been validated by various testing institutions and extensive comparisons of dummy kinematics with volunteers have been done revealing close correspondence. Therefore it is obvious to use this dummy for optimising the system.

Figure 10 shows a comparison of NIC values for BioRID and HIII(TRID) from tests with the two seat types mentioned above as well as the series seat to be optimised. Apparently, the values for the two dummies differ more and more as NIC increases. This is, however, not a generally valid conclusion /6/. The frame of the seat back is also decisive here. The series seat under investigation has a pronounced cross-member in the dummy's shoulder area. Since the HIII(TRID) has a rigid back structure, it does not detect this structure. The BioRID, on the other hand, has a back structure with a high level of biofidelity; the rigid frame in the seat back thus shows an effect in the area of the upper thoracic vertebra and causes

greater deceleration there, thus resulting in a higher NIC. As a remark, seats also exist for which the BioRID generates lower NIC values /6/. These seats have back rests being highly rigid along the sides, e.g. bucket seats. The HIII(TRID) has a rigid shoulder structure and therefore cannot sink back into the bucket seat. In the BioRID, the shoulders are flexible so that the dummy sinks back into the structure, resulting in a lower level of thorax deceleration and earlier head / headrest contact. Both factors reduce the NIC.

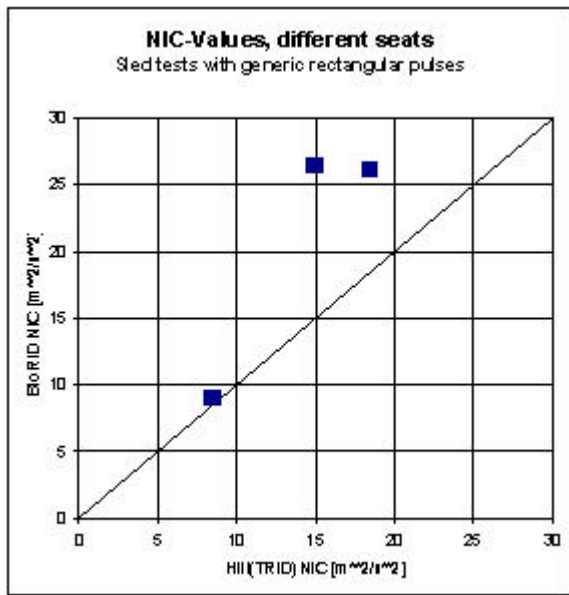


Fig. 10: Comparison of BioRID and HIII(TRID), three different seat types.

4. OPTIMISATION OF THE SYSTEM

The goal is to determine the optimum parametric curve for the deformation element in the AWS. Figure 11 shows the time history for the thorax and head acceleration in the series seat. The NIC value is determined in the first 80 ms mainly by the difference between these two factors. The aim is therefore to reduce thorax acceleration. Figure 12 shows the same test with already optimised AWS. Here the system is triggered at approx. 75 ms and thorax acceleration does not continue to increase, but instead remains nearly constant. Figure 13 shows the resulting influence on the NIC. It is reduced by the AWS from 26.3 to 17.6, i.e. by 9 points or 30%. It should also be mentioned at this point that head acceleration was also clearly reduced by the AWS, see Fig. 12.

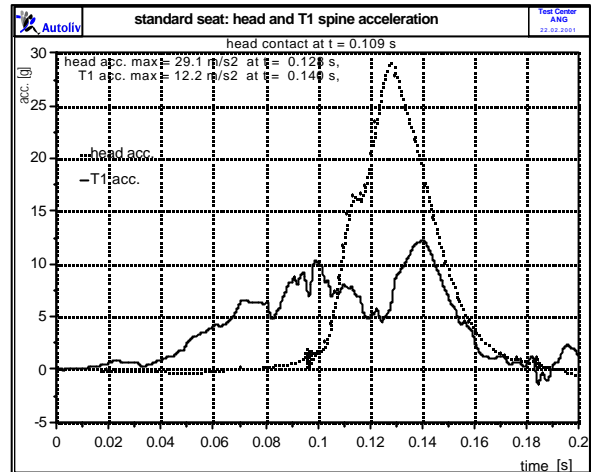


Fig. 11: Head and thorax acceleration, series seat

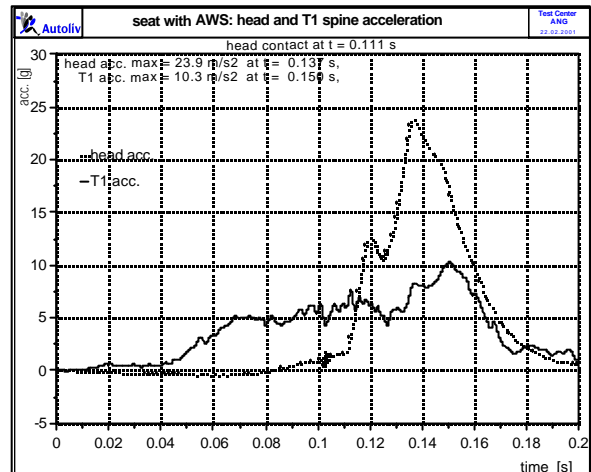


Fig. 12: Head and thorax acceleration, with AWS

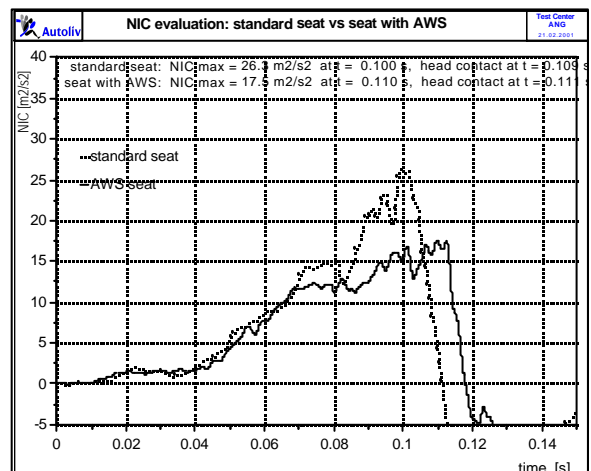


Fig. 13: NIC values with and without AWS

A further reduction of the NIC could be achieved by designing the trigger rivet to release at a lower force level. Since however everyday loads must also be taken into account, it is not possible to lower this release force threshold.

In further tests, the seat was tested with and without AWS at Δv 9 km/h and a 4 g rectangular pulse and at Δv 5 km/h with 3 g. The latter test was to make sure the system does not activate in minor accidents. At 9 km/h, on the other hand, release should take place, since CSD injuries can be expected beginning at this speed change level. In the 9 km/h test, a slight reduction of NIC is seen from 16.3 to 14.0, the system did activate (i.e. release), but the deformation element deformed in the front section only. This test shows that the efficiency of the AWS begins at this speed level. With AWS within a range of Δv 9 km/h to Δv 15 km/h the NIC value increases only slightly (see Fig. 14.).

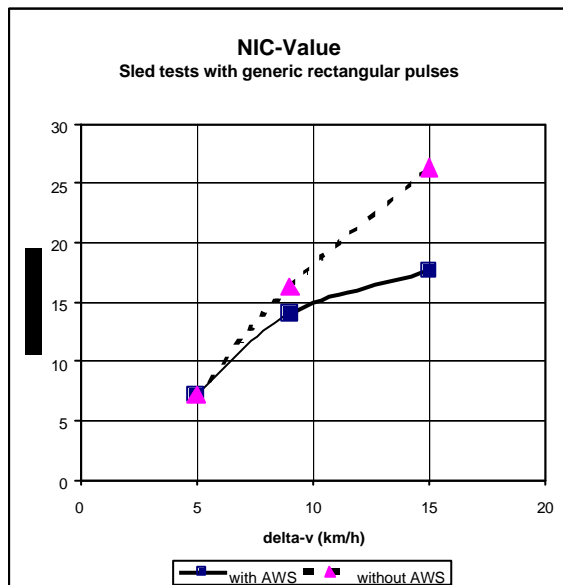


Fig. 14: Seat with and without AWS, NIC values at different speeds

To specify the utility of our AWS in more detail, extensive Madymo simulation were carried out.

5. SIMULATION

5.1 Simulation of rear impact with MADYMO - Computer simulation has been an essential tool in restraint system development for many years now. It was therefore decided to construct a simulation model for the load case "rear impact". The software program MADYMO was used, since a very good

BioRID_I mathematical model was already available at Autoliv /7/.

As the latest rear impact tests at Autoliv were done using a dummy, that has been introduced to advance development (BioRID_II), it was necessary to also enhance the software model of the dummy. For this purpose, the neck of the BioRID_I model was readapted to the behaviour of the BioRID_II in respect to elasticity and damping. The modified BioRID_I model shows an improved reality-like behaviour in the region of the cervical spine, thus making it possible to simulate head and T1 acceleration as well as the NIC (Neck Injury Criteria) at a high level of reliability. The typical S-shape of the neck occurring during rear impacts was achieved with this neck model as well.

5.2 Correlation to the test without AWS - A step-by-step procedure was employed in the correlation of the MADYMO model to the test.

First, the model - comprising the vehicle environment, seat and modified BioRID_I model - was correlated to a rear impact test ($\Delta v=15\text{km/h}$, 6g) including a series seat, i.e. without AWS. The adjusted parameters were in particular the seat frame stiffness, the contact characteristic between the dummy and the seat back, the intrusion stiffness of the head into the headrest and - the most important parameter to influence the neck loading - the rotational stiffness of the seat back round the y-axis.

The resulting model reproduces the head and the T1 accelerations in the x-direction well. It can also reproduce the measured NIC value well, both in the amplitude and in the time curve. The results are shown in Figs. 15 - 17.

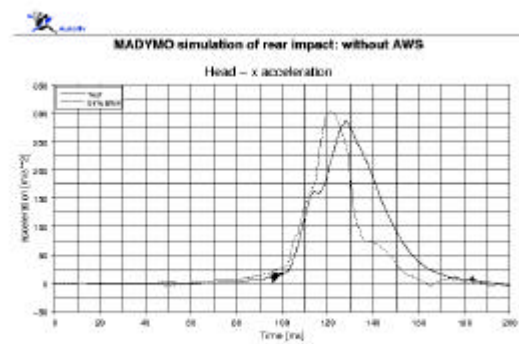


Fig. 15: head x-acceleration vs. time of seat system without AWS

In a rear collision, a relative movement between head and thorax occurs at between 50 ms and 110 ms, since the thorax is already accelerated by the seat

back at this point, but the head is still in the "free flight" phase. This can be seen in Figs. 15/16 also .

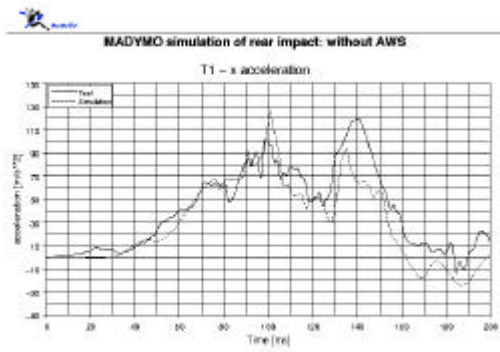


Fig. 16: T1 x-acceleration vs. time of seat system without AWS

At $t = 101$ ms the maximum of the T1 acceleration occurs, whereas the head experiences only little acceleration at this point. This difference in the acceleration values, finally, results in the high NIC value of approximately 26.

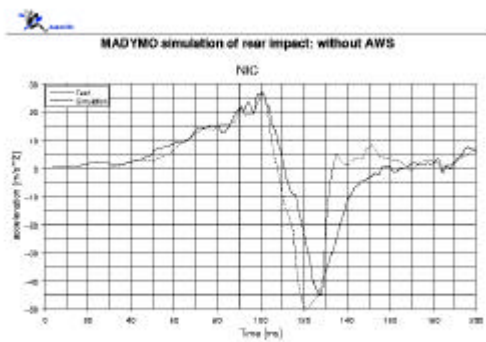


Fig. 17: NIC vs. time of seat system without AWS

The kinematic of the dummy in the system without AWS is shown in Figs. 18 – 20.



Fig. 18: Rear impact without AWS at $t = 60$ ms



Fig. 19: Rear impact without AWS at $t = 92$ ms



Fig. 20: Rear impact without AWS at $t = 120$ ms

5.3 Correlation of the model to the test with AWS

In the next step the MADYMO model was supplemented by the AWS.

The defined backward movement of the seat, which is made possible by the AWS (translation and rotation), significantly reduces the T1 acceleration in the x-direction thus resulting in a smaller difference between the head and the T1 acceleration. The characteristic curve "force vs. displacement" of the modelled AWS is adapted so that a correct AWS movement results. The correlated system generates, as in the test, a NIC value of approximately 16, i.e. considerably below the value of the system without AWS.

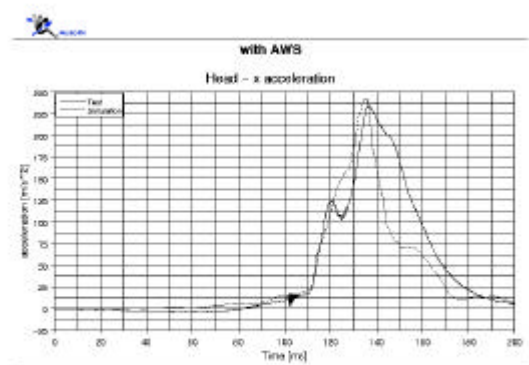


Fig. 21: head x-acceleration vs. time of seat system with AWS

With the system described here using AWS, it is possible to lower the maximum of the T1 acceleration in the x-direction from 13 g to 8 g. In Fig. 22 it can be seen that the “T1 x-acceleration vs. time” approximates a rectangular form. The thorax is here accelerated more evenly than without AWS, since the AWS allows for an optimum backward motion. The NIC can be reduced by over 30%.

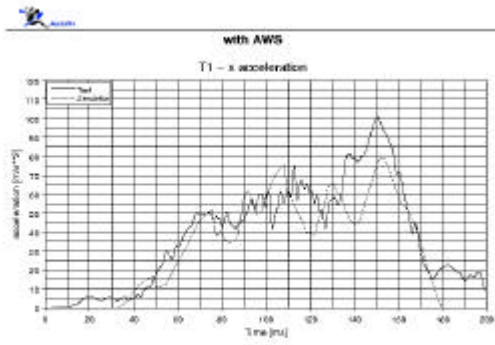


Fig. 22: T1 x-acceleration vs. time of seat system with AWS

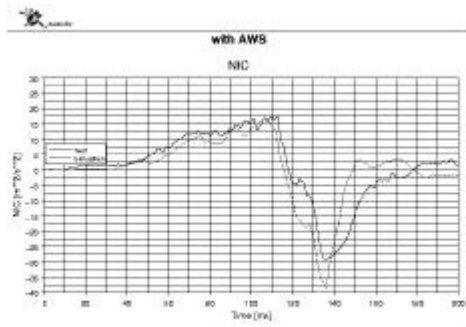


Fig. 23: NIC value vs. time of seat system with AWS

The changed kinematic during rear impact with AWS is seen in Fig. 24 - 27.

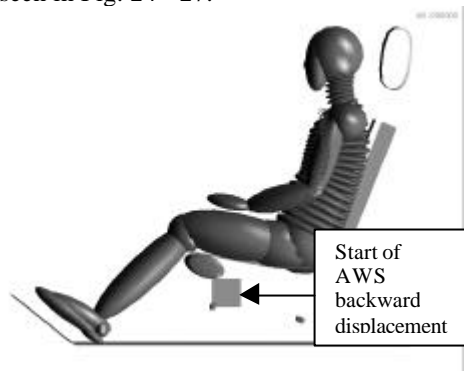


Fig. 24: Rear impact with AWS at t = 60 ms

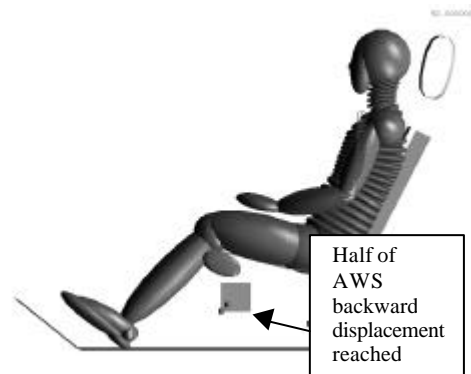


Fig. 25: Rear impact with AWS at t = 96 ms

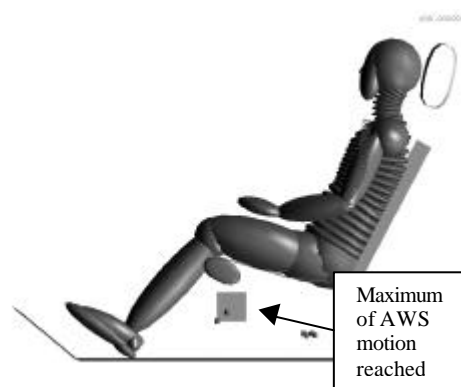


Fig. 26: Rear impact with AWS at t = 108 ms



Fig. 27: Rear impact with AWS at t = 120 ms

5.4 Modelling and optimisation of the AWS - In order to investigate the main influence of the deformation characteristic of the AWS on the dummy neck load values, a parametric study was carried out. The correlated simulation model for rear impact (see chapter 5.3) allows for a low-cost optimum design of the AWS in the environment of the correlated operating point. The range of reliability for a parametric variation, while retaining prognostic accuracy in this model, is estimated to be +/- 20 %.

The parameters were varied as follows:

Parameter	Range of variation
Force level of the AWS	+20 % / -20 %
Additional available displacement of the AWS	+ 5mm, +10mm, +15mm

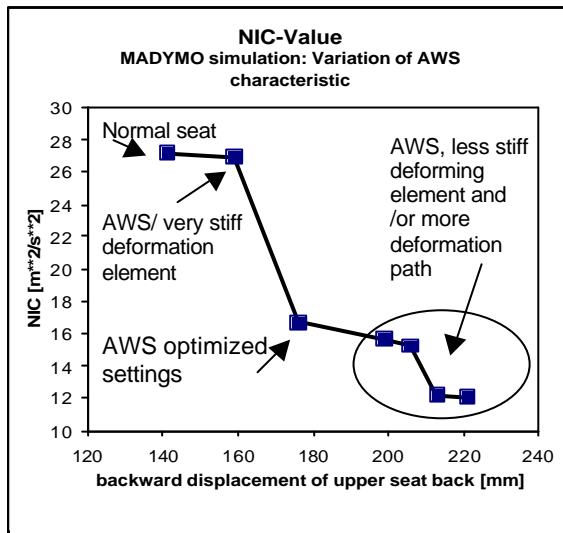


Fig. 28: Variation of AWS settings

Assuming the basic configuration, the force level for the AWS during the backward movement phase was varied. The force level of the deformation element is, however, the optimum compromise between NIC and rearward displacement of the seat (Fig. 28).

5.5 Variation of Δv - The AWS must solve a number of problems. It must protect the driver in an optimum manner for as wide a range as possible of Δv . At the same time the AWS should not release at too low speeds. In particular, the forces applied to the seat back in a so-called “daily use” must not activate the system, for instance rear-seat passengers getting in and out, whereby they hold onto the front seat.

To evaluate the performance capacity of the AWS, the influence on the dummy NIC value at various speeds Δv is to be determined.

Generic pulses – Fig. 29 shows the NIC value resulting from applying generic rectangular pulses to the simulation model. It can be seen clearly that the AWS motion threshold is at approx. $\Delta v = 9$ km/h. Up to $\Delta v = 16$ km/h the NIC value remains at a low level of about 16 and does not increase until higher

impact energies are applied, whereby the absolute improvement factor compared with the system without AWS is retained.

Improvement of the NIC value by installing AWS can be demonstrated up to $\Delta v = 20$ km/h. Raising Δv to above 20 km/h makes little sense since the BioRID was designed for low-speed impact and the biofidelity at higher Δv appears insufficient.

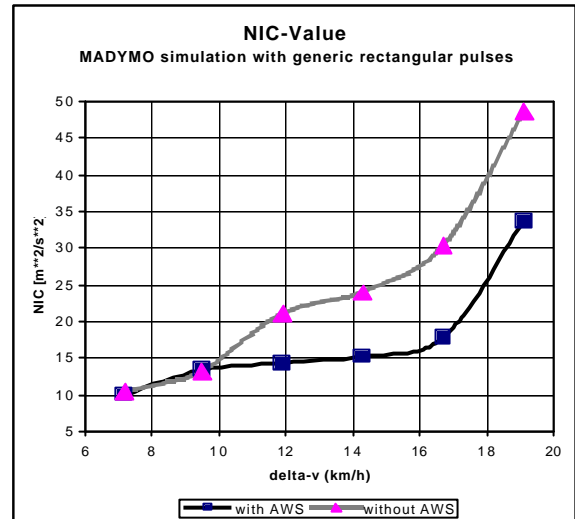


Fig. 29: NIC value vs. Δv (generic pulses)

The following table shows the relationship between Δv and the maximum of the generic pulse:

Δv [km/h]	Maximum of rectangular pulse [g]
7.2	3
9.5	4
11.9	5
14.3	6
16.7	7
19.1	8

Real crash pulses - The pulses used in a further study (Fig. 30) are from crash tests carried out by *Winterthur Accident Research*. Some of the data are from an offset crash configuration, which result in different energy input into the system than a 100% overlap crash. Therefore the neck loading can be different even if Δv is constant. The simulation shows that an AWS can reduce the NIC value by up to 38 %, even using real crash data, within the range of Δv from 11.5 km/h to 14.5 km/h.

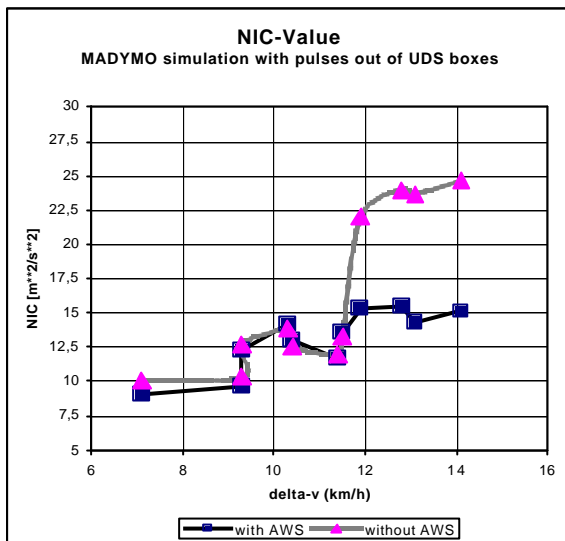


Fig. 30: NIC value over Δv (real crash pulses)

What can be noticed in particular is the shift of the activation threshold compared with systems to which generic pulses were applied. The reason for this is that the real pulses show a more gentle rise than the generic rectangular pulses. In Fig. 31 the generic pulse is compared to a corresponding real crash pulse ($\Delta v=14.1\text{km/h}$).

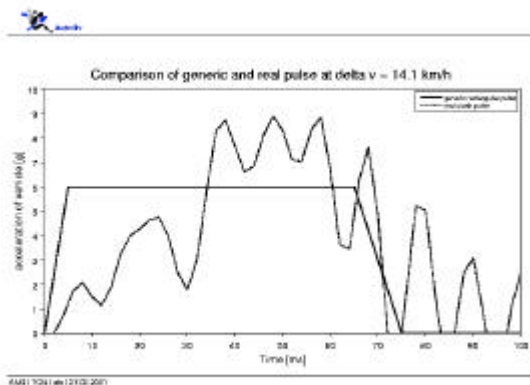


Fig. 31: generic and real pulse for $\Delta v = 14.1 \text{ km/h}$

6. CONCLUSIONS

Within the framework of this study, a prognostic Madymo Software Module was developed for the BioRID II, which is also available for further testing. The simulation shows that the design of the system represents an optimum compromise between reduction of the NIC and backwards seat movement. The AWS ensures nearly constant NIC in the Δv

range from 9 km/h to 17 km/h, i.e. in the speed range in which CSD injuries occur most frequently. The NIC values in this range are reduced by up to 30% and more. The AWS has now been developed for one vehicle type as far as the production maturity stage and will be going into production soon.

Our study shows the benefit of controlled energy absorption in the seat back in terms of reducing neck loading. Once this concept is used in a new seat design, further potentials for improvement are opened up, since the structure of the seat back can be optimised together with the deformation element. Further, release of the deformation element can be realised by means of an acceleration sensor instead of a trigger rivet. This would solve the conflict between robustness under everyday loads and optimum deformation characteristics in rear impact.

REFERENCES

/1/ Langwieder, K.; Hell, W.; Schick, S.; Muser, M.; Walz, F.; Zellmer, H.: Evolution of a Dynamic Seat Test Standard Proposal for a Better Protection after Rear-end Impact. IRCOBI Conference, Montpellier 2000.

/2/ Lundell, B.; Jakobsson, L.; Alfredsson, B.; Jernstrom, C.; Isaksson-Hellman, I.: Guidelines for the Design of a Car Seat Concept for Improved Protection Against Neck Injuries in Rear-end Car Impacts. SAE International Congress and Exposition, Detroit 1998.

/3/ Davidsson, J.; Svensson, M.Y.; Flogård, A.; Håland, Y.; Jakobsson, L.; Linder, A.; Lövsund, P.; Wiklund, K.: BioRID I—A new biofidelic rear impact dummy. IRCOBI Conference, Gothenborg 1998.

/4/ Ishikawa, T.; Okano, N.; Ishikura, K.; Ono, K.: An Evaluation of Prototype Seats Using BioRID-P3 and Hybrid III with TRID Neck. IRCOBI Conference, Montpellier 2000.

/5/ Muser, M.; Walz, F.; Zellmer, H.: Biomechanical Significance of the Rebound Phase in Low Speed Rear End Impacts. IRCOBI Conference, Montpellier 2000.

/6/ Zellmer, H.; Stamm, M.; Muser, M.; Walz, F.; Hell, W.; Langwieder, K.: to be published.

/7/ Eriksson, L.; Boström, O.: Assessing the influence of crash pulse, seat force characteristics, and head restraint position in NIC in rear-end crashes using a mathematical BioRID dummy. IRCOBI Conference, Barcelona 1999.